

# Dependence of exchange anisotropy and coercivity on the Fe-oxide structure in oxygen-passivated Fe nanoparticles

C. Prados, M. Multigner, and A. Hernando<sup>a)</sup>

*Instituto de Magnetismo Aplicado, UCM-RENFE. Box 155, 28230 Las Rozas, Madrid, Spain*

J. C. Sánchez and A. Fernández

*Departamento de Química Inorgánica, ICMS, CICIC, Avda A, Vespucio, Sevilla 41092, Spain*

C. F. Conde and A. Conde

*Departamento de Física de la Materia Condensada, US-ICMS, P.O. 1065, Sevilla 41080, Spain*

Ultrafine Fe particles have been prepared by the inert gas condensation method and subsequently oxygen passivated. The as-obtained particles consist in an Fe core surrounded by an amorphous Fe-oxide surface layer. The antiferromagnetic character of the Fe-oxide surface induces an exchange anisotropy in the ferromagnetic Fe core when the system is field cooled. Samples have been heat treated in vacuum at different temperatures. Structural changes of the Fe-O layer have been monitored by x-ray diffraction and transmission electron microscopy. Magnetic properties as coercivity, hysteresis loop shift, and evolution of magnetization with temperature have been analyzed for different oxide crystallization stages. A decrease of the exchange anisotropy strength is reported as the structural disorder of the surface oxide layer is decreased with thermal treatment.

© 1999 American Institute of Physics. [S0021-8979(99)38808-3]

## INTRODUCTION

Magnetic fine particles have traditionally attracted intense research interest.<sup>1</sup> They exhibit a number of physical phenomena related to the so-called size effects. Beside the interest in understanding the nature and mechanisms of such new phenomena, there is a technological driven force due to the immediate applications of these systems, mainly in high-density magnetic recording media.<sup>2</sup> Some of these outstanding phenomena accompanying the size reduction are related to the transition to a single-domain magnetic structure, for instance, superparamagnetism,<sup>3</sup> large coercivities,<sup>4</sup> quantum tunneling of magnetization,<sup>5</sup> giant magnetoresistance,<sup>6</sup> etc. New methods of synthesis (inert gas condensation, layer deposition, mechanical attrition, aerosol) allow not only fabricating magnetic systems with characteristic dimensions on the nanometer scale, but also producing heterogeneous magnetic materials in a controlled compositional and structural manner. An example of these heterogeneous systems are the passivated nanoparticles, in which a metallic inner core is surrounded by an oxide shell. Combination of a ferromagnetic metallic core and an antiferromagnetic oxide shell leads, after a field-cooling process, to the apparition of a magnetic unidirectional anisotropy named exchange anisotropy.<sup>7</sup> The main effect of such an anisotropy is the occurrence of a displacement in the hysteresis loop of the coupled system, labeled as exchange biasing. Recent experiments point out the role of the spin disorder at the interface in the origin of this unidirectional anisotropy in antiferromagnetic-layered structures<sup>8</sup> and in homogeneous<sup>9</sup> and passivated nanoparticles.<sup>10</sup> In this article, attention has been focused on the evolution of the magnetic behavior of exchange-coupled passivated Fe nanoparticles with the struc-

tural modification of the oxide shell. A decrease of the strength of the exchange anisotropy is observed as the external oxide shell is ordered.

## EXPERIMENT

Nanocrystalline Fe particles have been prepared by evaporation of pure Fe in a tungsten boat at 1500 °C. A helium atmosphere was kept during deposition at a pressure of 133 Pa (1 Torr). Evaporated atoms lose kinetic energy through interatomic collisions with the inert gas, and condense as an ultrafine powder, which is collected on a cold finger.<sup>11</sup> Shell passivation was achieved by dosing oxygen (266 Pa for 10 min). Subsequent heat treatments of the passivated particles were performed under high vacuum ( $10^{-7}$  Torr) during 4 h at a fixed temperature. The different annealing processes are labeled with these typical temperatures, which were varied up to 300 °C.

Transmission electron microscopy (TEM) was performed using a Philips CM200 microscope working at 200 kV. Figure 1 shows a TEM micrograph of the passivated ultrafine powder. The material consists of nanometric particles in which the shell-core structure is clearly visible. The dark inner core is the metallic iron, whereas the lighter surrounding layer corresponds to the oxide phase.

Powders have also been structurally characterized by means of x-ray diffraction (XRD) analysis. Figure 2 shows a typical XRD pattern corresponding to the sample annealed at 250 °C. It reveals the presence of pure  $\alpha$ -Fe and nanocrystalline Fe oxide (either  $\gamma$ -Fe<sub>2</sub>O<sub>3</sub> or Fe<sub>3</sub>O<sub>4</sub>, since the slight difference in the lattice parameter of both compounds makes it extremely difficult to differentiate them). Crystalline sizes of the pure iron and the oxide phase have been estimated by means of the Debye-Scherrer formula.

<sup>a)</sup>Electronic mail: antonio@fenix.ima.csic.es

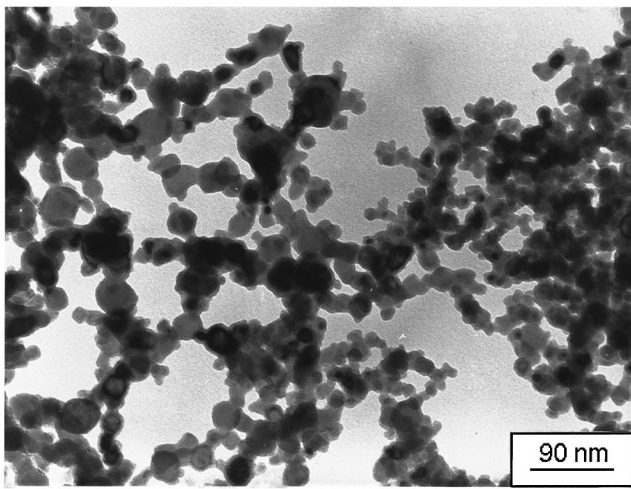


FIG. 1. TEM micrograph of the oxygen-passivated Fe powder.

The magnetic behavior of the sample and its evolution with the annealing temperature have been performed between 5 and 300 K in temperature by using a commercial semiconducting quantum interference device (SQUID) magnetometer supplying a maximum field of 55 kOe.

**RESULTS AND DISCUSSION**

The XRD patterns for the as-obtained sample reveals that the shell oxide species (Fe-O) are amorphous in the sense of the x-ray diffraction<sup>10</sup> (with a grain size lower than 2.5 nm, diffraction effects are diffuse and close to the background noise, therefore, when the crystalline coherence is lower than this value, the material is considered as amorphous in the sense of the x-ray diffraction). Figure 3 shows the increase of the Fe-O phase grain size as a function of the annealing temperature. Heat treatments have been carried out in a high-vacuum environment in order to enhance the crystalline order of the oxide shell preventing the metallic core from further oxidation. Magnetization at the maximum applied field (55 kOe) is also displayed in Fig. 3 as a function of the annealing temperature. The value of  $M_{55\text{ kOe}}$  is rather constant with a slight decrease for the maximum annealing

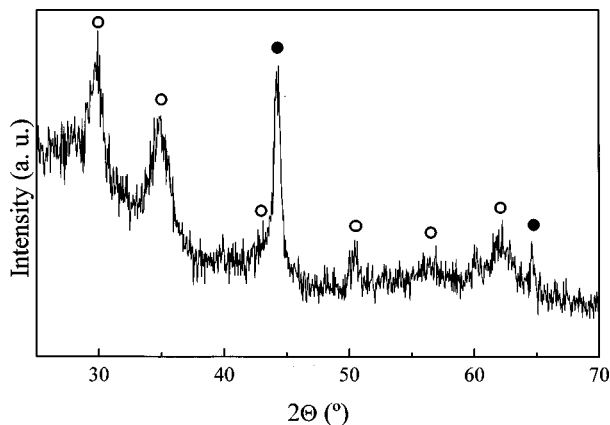


FIG. 2. X-ray diffractogram of the sample annealed in vacuum at 250 °C. Open circles indicate the position of the peaks corresponding to  $\gamma\text{-Fe}_2\text{O}_3$  and  $\text{Fe}_3\text{O}_4$ . Full circles indicate the  $\alpha\text{-Fe}$  peaks.

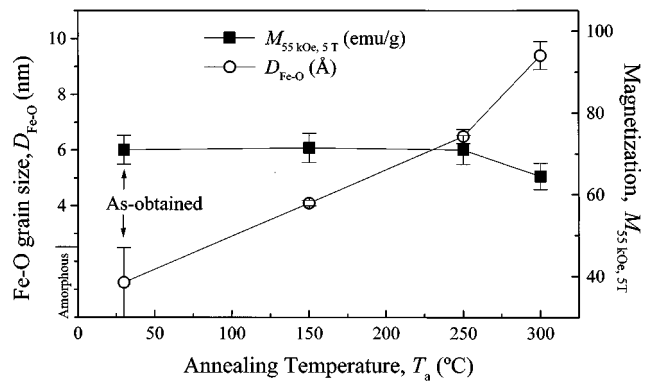


FIG. 3. Evolution of the Fe-O grain size and the magnetization at 55 kOe and 5 K with the annealing temperature.

temperature. This fact confirms that the intrinsic magnetic properties of the metallic core are essentially not affected by the annealing procedure.

Hysteresis loops for the as-obtained and annealed samples have been measured at 5 K following the conventional zero-field-cooling (ZFC) and field-cooling (FC) procedures. As expected, a shift towards negative fields have been observed in the FC hysteresis loops which did not appear after a ZFC process. It is originated by the exchange anisotropy induced on the ferromagnetic phase, when the composite antiferro-ferromagnetic system in cooled under an applied magnetic field across the Néel temperature of the antiferromagnetic phase. Figure 4 shows the evolution of the shift in the FC hysteresis loops (exchange field,  $H_{ex}$ ) as a function of the grain size of the Fe-O shell. The exchange field is monotonically decreasing as the structural order of the antiferromagnetic phase is enhanced. The exchange anisotropy has been phenomenologically well understood since the 1950s,<sup>7</sup> in the framework of an uncompensated spin structure at the antiferro-ferromagnetic interface. However, even nowadays there is little quantitative understanding of the underlying coupling mechanisms, which have been also observed in spin-compensated interfaces.<sup>12</sup> Recent experiments on layered<sup>8,13</sup> and particulate systems<sup>9,10,14</sup> demonstrate the influence of the interfacial magnetic disorder on the

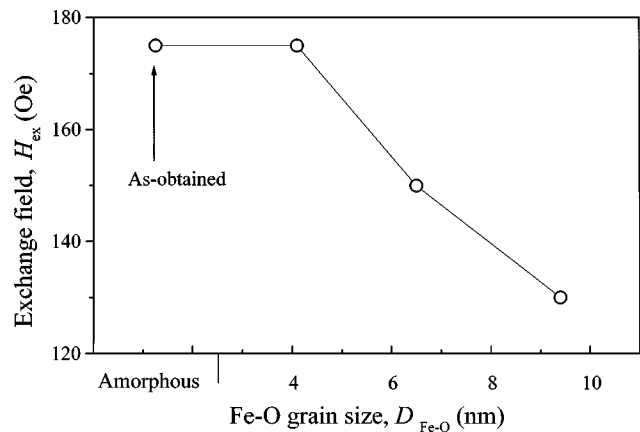


FIG. 4. Evolution of the exchange field with the grain size of the Fe-O shell.

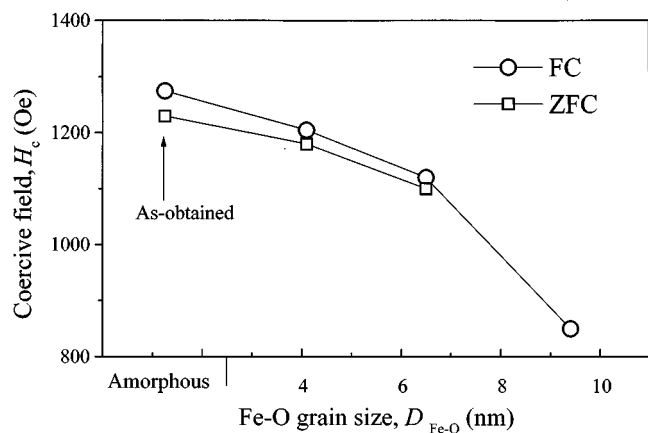


FIG. 5. Evolution of the ZFC and FC coercivity fields with the grain size of the Fe–O shell.

exchange anisotropy. In the as-obtained sample, the magnetic disorder related to the structural disorder of the amorphous Fe–O shell phase is in the origin of the observed exchange anisotropy.<sup>10</sup> As the Fe–O shell is crystallized by means of the subsequent heat treatments, the strength of the exchange coupling decreases as a consequence of the increase of the structural order. The slight decrease of the core saturation magnetization due to any eventual oxygen diffusion from the Fe–O phase towards the metallic core, could not explain the reduction of the exchange field, since  $H_{\text{ex}}$  depends on the inverse of the ferromagnetic saturation magnetization.<sup>15</sup>

Figure 5 shows the evolution of ZFC and FC coercivities with the Fe–O grain size at 5 K. Coercivity data follow a similar trend to that observed for  $H_{\text{ex}}$ . They decrease when the Fe–O grain size rises. The exchange interactions between the core magnetic moments, which are pinned by the frozen Fe–O shell, constitute an extra energy term in the magnetization switching. Therefore, as observed, there should exist a relation between coercivity and exchange anisotropy strength. We should point out that although the shifted hysteresis loops are detected only when the sample is field cooled, the individual particles are exchange coupled to their corresponding shell either after a FC or a ZFC process. It can be considered that, owing to the small size of the Fe particles, they are within the magnetic monodomain regime. Hence, each individual particle is magnetically saturated during either cooling process. The magnetization will be lying along the anisotropy easy axis of each particle in the case of ZFC or along the applied magnetic field in the FC process. In the first case, the induced unidirectional anisotropy axis will point randomly in each individual particle, as corresponds to the random distribution in sizes and orientation of the par-

ticles. The measured “macroscopic” hysteresis loop is the composition of the hysteresis loops of all individual particles. After a ZFC process, those particles with their anisotropy easy axes along the measurement direction will contribute with loops shifted towards either positive or negative directions. The particles with anisotropy axes perpendicular to the measurement direction will contribute with anhysteretic centered loops. In the FC case, there will be a single bias direction corresponding to that of the applied field, giving rise to the observed shift of the “macroscopic” hysteresis loop, since the loops of each individual particle are shifted towards the same direction. The reason for the different values of the ZFC and FC coercivities displayed in Fig. 5 is the anhysteretic behavior of the particles contributing with centered loops after a ZFC process.

## CONCLUSION

Passivated Fe fine particles with Fe–O shells in different crystallization stages have been obtained by means of controlled heat treatments. The occurrence of an exchange anisotropy effect between the ferromagnetic core and the Fe–O shell results in a shift of the FC hysteresis loops. The decrease of the exchange bias field with the heat treatment indicates that the strength of the induced unidirectional exchange anisotropy is decreasing as the structural order of the antiferromagnetic Fe–O phase is enhanced. This effect makes evident the role of the structural-magnetic disorder in the mechanism of the exchange anisotropy.

<sup>1</sup> *Magnetic Properties of Fine Particles*, edited by J. L. Dorman and D. Fiorani (North-Holland, Amsterdam, 1992).

<sup>2</sup> F. T. Parker, F. F. Spada, T. J. Cox, and A. E. Berkowitz, *J. Magn. Magn. Mater.* **162**, 122 (1996).

<sup>3</sup> I. S. Jacobs and C. P. Bean, in *Magnetism*, edited by G. T. Rado and H. Suhl (Academic, New York, 1963), Vol. 3, Chap. 6.

<sup>4</sup> E. F. Kneller and F. E. Luborsky, *J. Appl. Phys.* **34**, 656 (1963).

<sup>5</sup> E. M. Chudnovsky and L. Gunther, *Phys. Rev. Lett.* **60**, 661 (1988).

<sup>6</sup> J. Q. Xiao, J. S. Jiang, and C. L. Chien, *Phys. Rev. Lett.* **68**, 3745 (1992).

<sup>7</sup> W. H. Meiklejohn and C. P. Bean, *Phys. Rev.* **105**, 904 (1957).

<sup>8</sup> K. Takano, R. H. Kodama, A. E. Berkowitz, W. Cao, and G. Thomas, *Phys. Rev. Lett.* **79**, 1130 (1997).

<sup>9</sup> B. Martínez, X. Obradors, Ll. Balcells, A. Rouanet, and C. Monty, *Phys. Rev. Lett.* **80**, 181 (1998).

<sup>10</sup> L. del Bianco, A. Hernando, M. Multigner, C. Prados, J. C. Sánchez-López, A. Fernández, C. F. Conde, and A. Conde, *J. Appl. Phys.* **84**, 2189 (1998).

<sup>11</sup> H. Gleiter, *Prog. Mater. Sci.* **33**, 223 (1989).

<sup>12</sup> J. Nogués, D. Lederman, T. J. Moran, and I. K. Schuller, *Appl. Phys. Lett.* **68**, 3186 (1996).

<sup>13</sup> D. V. Dimitrov, S. Zhang, J. Q. Xiao, C. C. Hadjipanayis, and C. Prados, *Phys. Rev. B* **58**, 12090 (1998).

<sup>14</sup> R. H. Kodama, A. E. Berkowitz, E. J. McNiff, Jr., and S. Foner, *Phys. Rev. Lett.* **77**, 394 (1996).

<sup>15</sup> For an analytical description of the dependence of the exchange field on the saturation magnetization of the ferromagnetic phase see, for instance, W. H. Meiklejohn, *J. Appl. Phys.* **33**, 1328 (1962).